Analyses of photon breeding with respect to photon spin by using a three-dimensional quantum walk model

M. Ohtsu[1], E. Segawa[2], K. Yuki[3], and S. Saito[4]

[1]Research Origin for Dressed Photon,3-13-19 Moriya-cho, Kanagawa-ku, Yokohama, Kanagawa 221-0022, Japan

[2]Yokohama National University, 79-8 Tokiwadai, Hodogaya-ku, Yokohama, Kanagawa 240-8501, Japan

[3]Middenii, 3-3-13 Nishi-shinjuku, Sinjuku-ku, Tokyo 160-0023, Japan

[4]Kogakuin University, 2665-1, Nakano-machi, Hachioji, Tokyo 192-0015, Japan

Abstract

This article describes the features of photon breeding with respect to the photon spin of light emitted from a Si light-emitting diode by using a three-dimensional QW model. A relation between the direction of the linear polarization of the incident light and dressed photon hopping is assumed by referring to teachings from classical electromagnetics. Numerical calculations reveal that the dressed -photon–phonon creation probability at a B atom-pair depends on the polarization, and the degree of photon breeding is as large as 2%, which agrees with the experimentally confirmed value.

1. Introduction

A dressed photon (DP) is a quantum field created by the interaction between photons and electrons (or excitons) in a nanometer-sized particle (NP) or an atom under light irradiation. The created DP localizes at the NP or atom. It is an off-shell quantum field because its momentum has large uncertainty due to its subwavelength size [1, 2]. Furthermore, the DP couples with a phonon to create a new quantum field, named a dressed-photon–phonon (DPP).

The spatial distribution of a DPP created and confined at an impurity boron (B) atom-pair in a silicon (Si) crystal has been analyzed by using a two-dimensional quantum walk (QW) model [3]. This analysis found that the created DPP was efficiently confined by the B atom-pair when the pair was oriented along a direction perpendicular to that of the incident light propagation.

The observable on-shell field energy that leaked out to the macroscopic outer space has been experimentally measured [4]. This energy was generated due to the dissipation of the microscopic off-shell DPP field energy. For comparison with the experimental results, an energy dissipation constant κ was introduced in the two-dimensional QW model for detailed analysis of the DPP creation and confinement at a B atom-pair [4]. This analysis succeeded in describing the intrinsic features of the DPP energy transfer, dissipation, and the photon breeding (PB) with respect to the photon momentum.

As the next step in the QW analysis, the present article presents calculation results describing the PB with respect to the photon spin. Section 2 reviews experimental results to be analyzed. Section 3 presents a three-dimensional QW model used for the analysis. Section 4 describes the results of numerical calculations. Section 5 presents a summary.

2. Revisit of experimental results

It is widely known that the light emission efficiency of crystalline silicon (Si) is extremely low. However, revolutionary light-emitting diodes (LED) and lasers were invented recently by applying a novel fabrication method, named DPP-assisted annealing, to a Si crystal [5]. Briefly, this method is summarized as follows: After boron (B) atoms are doped in the Si crystal, the crystal is Joule-heated by current injection to allow diffusion of the B atoms. During this heating, the Si crystal is irradiated with light, resulting in the formation of B atom-pairs by autonomous control of their orientations and lengths.

After this fabrication by using DPP-assisted annealing, current injection to the device creates a DPP again at the B atom-pair, and this DPP serves as an efficient photon emitting source. As a result, the annealed Si crystal works as an LED or as a laser. Two epoch-making inherent feature of these devices were experimentally confirmed: PB with respect to the photon energy, and the photon spin (polarization) of the emitted light. That is, the generated light was a replica of the light irradiated during the DPP-assisted annealing. PB with respect to the photon energy has been quantitatively described by analyzing the relations among the energies of photons, excitons, and phonons [6]. Although experiments on PB with respect to the photon momentum have not yet been carried out, numerical calculations using a QW model have reproduced its feature [3].

The present article reports the results of numerical analyses of PB with respect to the photon spin by using a QW model. Relevant experimental results on Si-LEDs, to be analyzed here, are summarized as follows [7,8]: Although the method of fabrication was equivalent to the one reviewed above, linearly polarized light was used for the DPP-assisted annealing. After fabrication, a current was injected to the device for LED operation. The degree of polarization* P of the emitted light was found to be nonzero at the photon energy $h\nu_{anneal}$ of the light irradiated for the DPP-assisted annealing. The value of P increased by increasing the DPP-assisted annealing time and saturated to 7×10^{-2} (=7 %). Furthermore, the relation between the number of the B atom-pairs and the azimuthal angle φ of orientation were measured, where $\varphi=0^\circ$ corresponded to the polarization direction of the light irradiated during the annealing. This number increased with increasing φ and took the maximum at $\varphi=90^\circ$ (the angle normal to the direction of the electric field of the linearly polarized light). This angular dependence indicated that the diffusion of the B atoms was controlled by the linearly polarized light irradiated during the DPP-assisted annealing, resulting in autonomous orientation of the B atom-pairs to the direction of $\varphi=90^\circ$.

==========

(*) Degree of polarization is defined as $P \equiv \left(I_{\parallel} - I_{\perp}\right) \Big/ \left(I_{\parallel} + I_{\perp}\right)$, where $I_{\parallel}$ is the intensity of the linearly polarized light under evaluation. $I_{\perp}$ is that of the light whose polarization direction is normal to that of $I_{\parallel}$ [a].

[a] M. Born and E. Wolf, Principles of Optics, Fourth edition (Pergamon Press, Oxford, 1970) p.45.

==========

The experimental results above confirmed that the light emitted from the fabricated Si-LED was polarized, and the polarization direction was governed by that of the light irradiated during the DPP-assisted annealing, that is to say, PB with respect to the photon spin. There are two possible origins of the induced photon spin [7,8]:

(1) The B atom-pair serves as a nanometer-sized wire-grid in the xy-plane of Fig. 1 (the orientation of this grid is φ=90°). Classical electromagnetics teaches that the light emitted from the wire-grid is linearly polarized along the direction (φ=0°) that is parallel to the electric field of the light irradiated during the DPP-assisted annealing. As a result, the polarization direction of the emitted light becomes identical to that of this irradiated light.

(2) By the DPP-assisted annealing, a transverse optical phonon is created and couples with the DP at the B atom-pair [9-11]. The vibration direction of this phonon is parallel to that of the electric field of the polarized light (φ=0°) that is irradiated during the DPP-assisted annealing. When this LED is used as a light emitter, this phonon is created again by current injection, and the direction of the electric field vector of the emitted light also becomes parallel to the vibration direction of the phonon. Thus, the polarization direction of the emitted light becomes identical to that of the light irradiated during the DPP-assisted annealing.

The number of B atom-pairs for $\varphi \geq 45°$ was 8×10^{-2} (=8 %) [7,8] of the total number, which is nearly equal to the saturated value of P (=7×10^{-2} (=7 %)) presented above [7,8]. This agreement supports the origins (1) and (2) above. For comparison, the light emitted from conventional LEDs fabricated by using composite semiconductor crystals is non-polarized, i.e., P is zero.

The phenomenon to be analyzed in the present study is schematically summarized in Fig. 1, by referring to the experimental results above. Here, the light propagates along the z-axis and is incident on the Si crystal, as was the case of the light irradiated during the DPP-assisted annealing. It is assumed that the B atom-pair orients along the x-axis because from experiments it was found that the DPP creation probability at this pair is higher than the case when it is oriented along the z-axis. Numerical analyses using a QW model have confirmed that this assumption was adequate [3].

Furthermore, as shown in Fig. 1(a), the incident light is assumed to be linearly polarized along the y-axis. Experiments have confirmed that this polarized light realized higher creation/confinement probability of the DPP at the B atom-pair compared with the case of light linearly polarized along the

x-axis (Fig. 1(b)) [7,8]. The goal of the present study is to reproduce this experimental confirmation by numerical calculations .

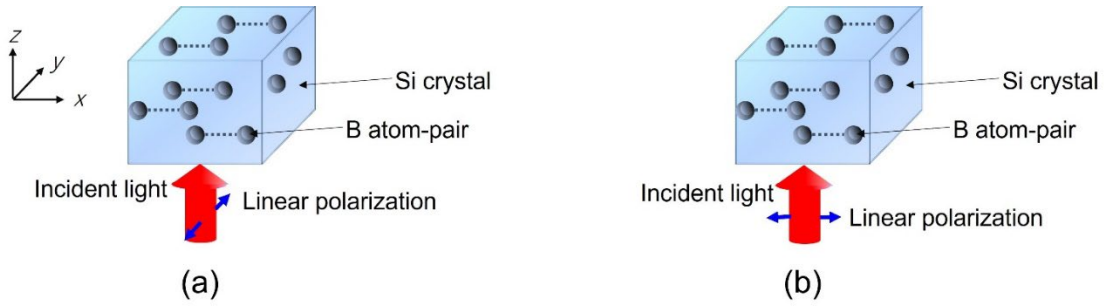

Fig.1 Relations among the directions of the orientation of a B atom-pair (along x-axis), the incident light propagation (z-axis), and its polarization.
(a) and (b) are for the linear polarization along y- and x-axes, respectively.

3. Three-dimensional quantum walk model

Figure 2 represents a three-dimensional lattice that in used as the three-dimensional QW model of the Si crystal. Blue squares represent the sites of Si atoms. Two red squares represent a B atom-pair at the center of the lattice. By referring to the calculated result in ref. [3], it is assumed that this pair orients along the x-axis, and its length d is three times the lattice constant a of the Si crystal ($d = 3a$).

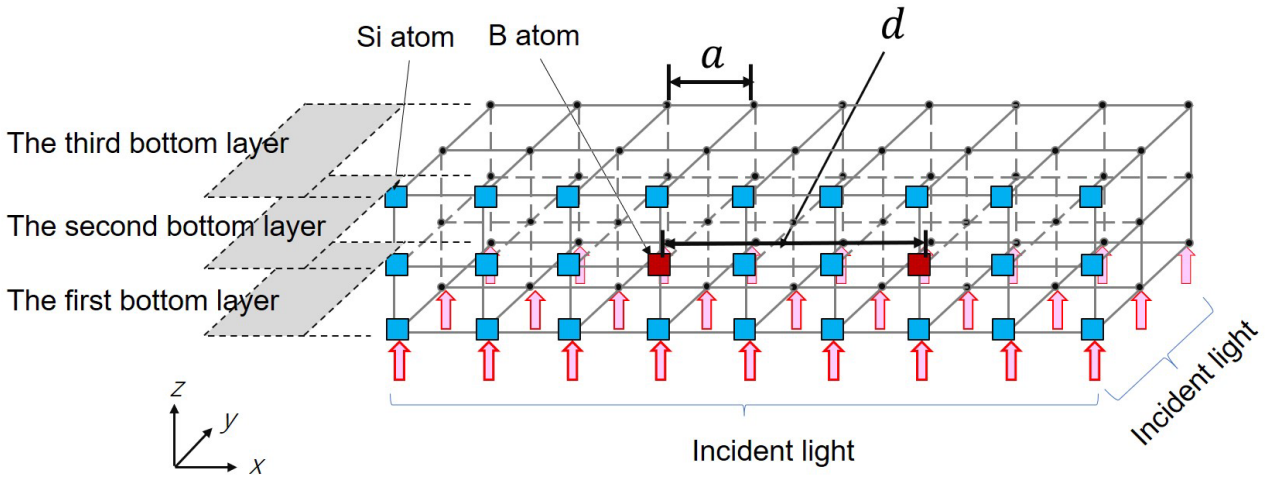

Fig. 2 Structure of a three-dimensional lattice.
Blue and red squares represent the sites of the Si and B atoms, respectively. The length d of the B atom-pair, oriented along the x-axis, is $d = 3a$, where a is the lattice constant of the Si crystal.

For comparison, Fig. 3 represents the two-dimensional lattice that was used in the previous studies [3,4]. DPP energy transfers in the upper-right and lower-left directions, as represented by red

and blue broken arrows in Fig. 3(a). These transfers originate from the repetitive hopping of the DP from one site to its nearest-neighbor, as represented by red and blue bent arrows for the sites A (Fig. 3(b)) and B (Fig. 3(c)). Since the phonon does not hop, it is represented by a closed loop. In the case of the three-dimensional lattice, the bent arrows in Figs. 3(b) and (c) are replaced by red and blue bent arrows in Fig. 4. The senses of the repetitive DP hopping in Figs. 4(a) and (b) are those of advancing right-handed and left-handed screws, respectively. They correspond to modes 12 and 1, respectively, in ref. [12].

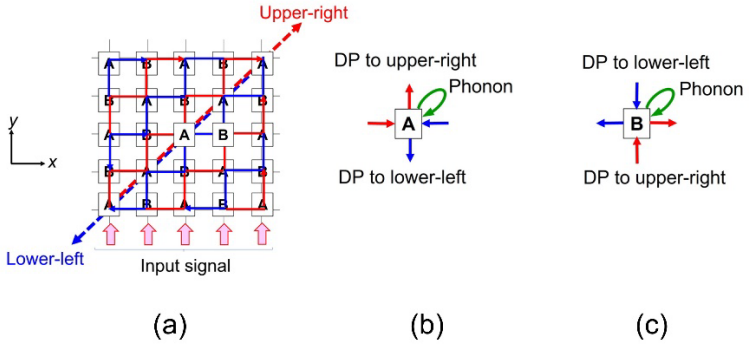

Fig. 3 Structure of a two-dimensional lattice.

(a) The overall profile. Red and blue bent arrows in (b) and (c) represent the DP hopping to/from sites A and B, respectively. The phonon is represented by a green closed loop.

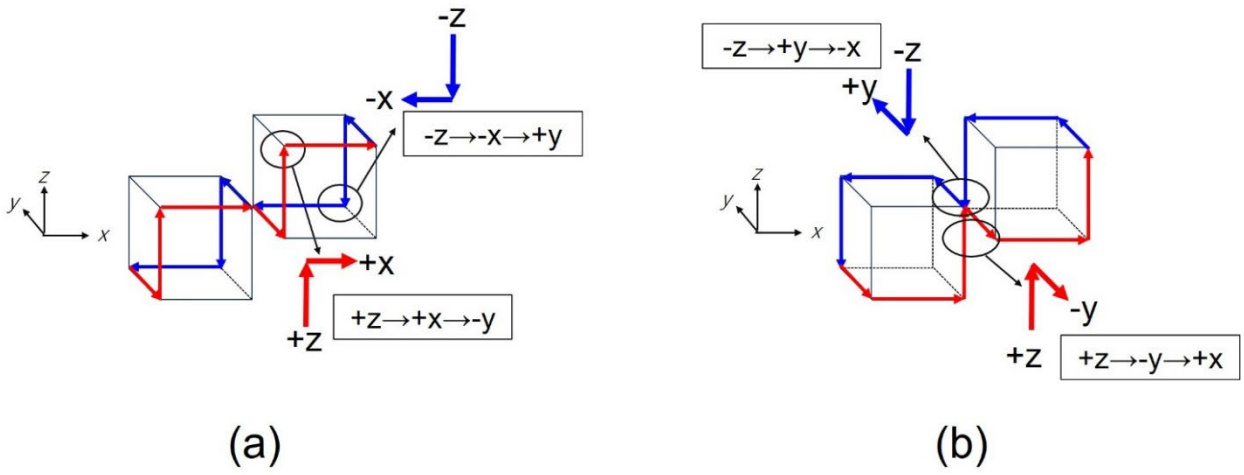

Fig. 4 DP hopping from one site to its nearest-neighbor in the three-dimensional lattice.

(a), (b) The senses of the repetitive DP hopping are those of advancing right-handed and left-handed screws, respectively.

DP is created at each site on the first bottom layer (Fig. 2) of the three-dimensional lattice by the incident light that propagates along the $+z$-axis. The created DP subsequently hops to the nearest-neighbor site. In order to introduce the polarization of the incident light in the QW model, first, the case of linear polarization along the y-axis (Fig. 1(a)) is dealt with. Since the electric field of this light oscillates along the y-axis, classical electromagnetics teaches that this electric field creates an

electric dipole in the NP or atom that oscillates also along the y-axis (Fig. 5(a)). This oscillating dipole emits an electromagnetic field that propagates along the x-axis. This emission process is equivalent to that of the emission from the nanometer-sized wire-grid in (1) in Section 2. Thus, it can be assumed that the DP on the first bottom layer of the three-dimensional lattice hops along the x-axis (the first step in Fig. 6(a)). Here, since the incident light is an alternating electromagnetic field, it should be noted that the DP hops not only in the $+x$-axis direction but also in the $-x$-axis direction, alternately in time. By following red arrows in Fig. 4(a), the DP subsequently hops along the y- and z-axes (the second and third steps, respectively, in Fig. 6(a)). In the third step, by hopping along the z-axis, the DP transfers energy from the sites in the first bottom layer to those in the second bottom layer. By repeating this hopping, DP energy transfers from the lower to the upper layers of the three-dimensional lattice and reaches the B atom-pair. Since hopping along the $-y$-axis and $-z$-axis is also allowed, as was the case of the $-x$-axis above, the transfers from the upper to the lower layers are represented by blue arrows in Fig. 4(a).

Second, in the case of the incident light with linear polarization along the x-axis (Fig. 1(b)), the created electric dipole oscillates also along the x-axis, and the emitted electromagnetic field propagates along the y-axis (Fig. 5(b)). Thus, the DP starts hopping along the y-axis (the first step in Fig. 6(b)). Figure 6(b) also shows subsequent hopping of the second and third steps.

Numerical calculations were carried out to derive the stationary value of the creation probability of the DPP at the B atom-pair after repeating the DP hopping in Fig. 6. Since the B atom-pair in Fig. 1(a) orients along the x-axis, it is expected that the calculated value of the DPP creation probability in Fig. 6(a) is larger than that in Fig. 6(b), as was experimentally confirmed in Section 2.

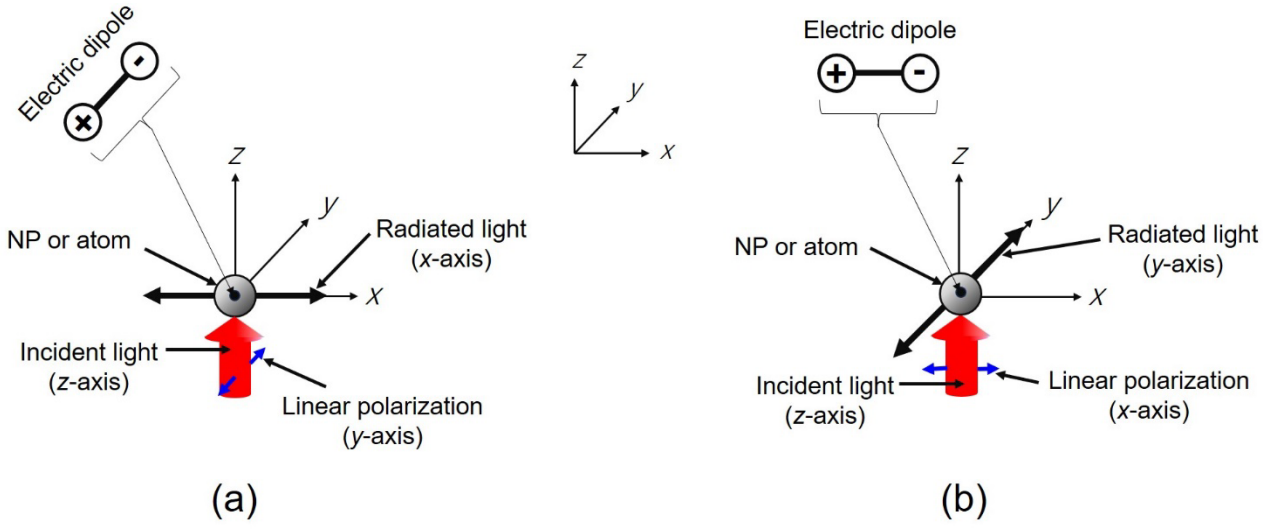

Fig. 5 Relations among the directions of the incident light propagation (z-axis), its polarization, and the light propagation emitted from the electric dipole in a nanometer-sized particle (NP) or an atom.
(a) and (b) are for the incident light that is linearly polarized along y- and x-axes, respectively.

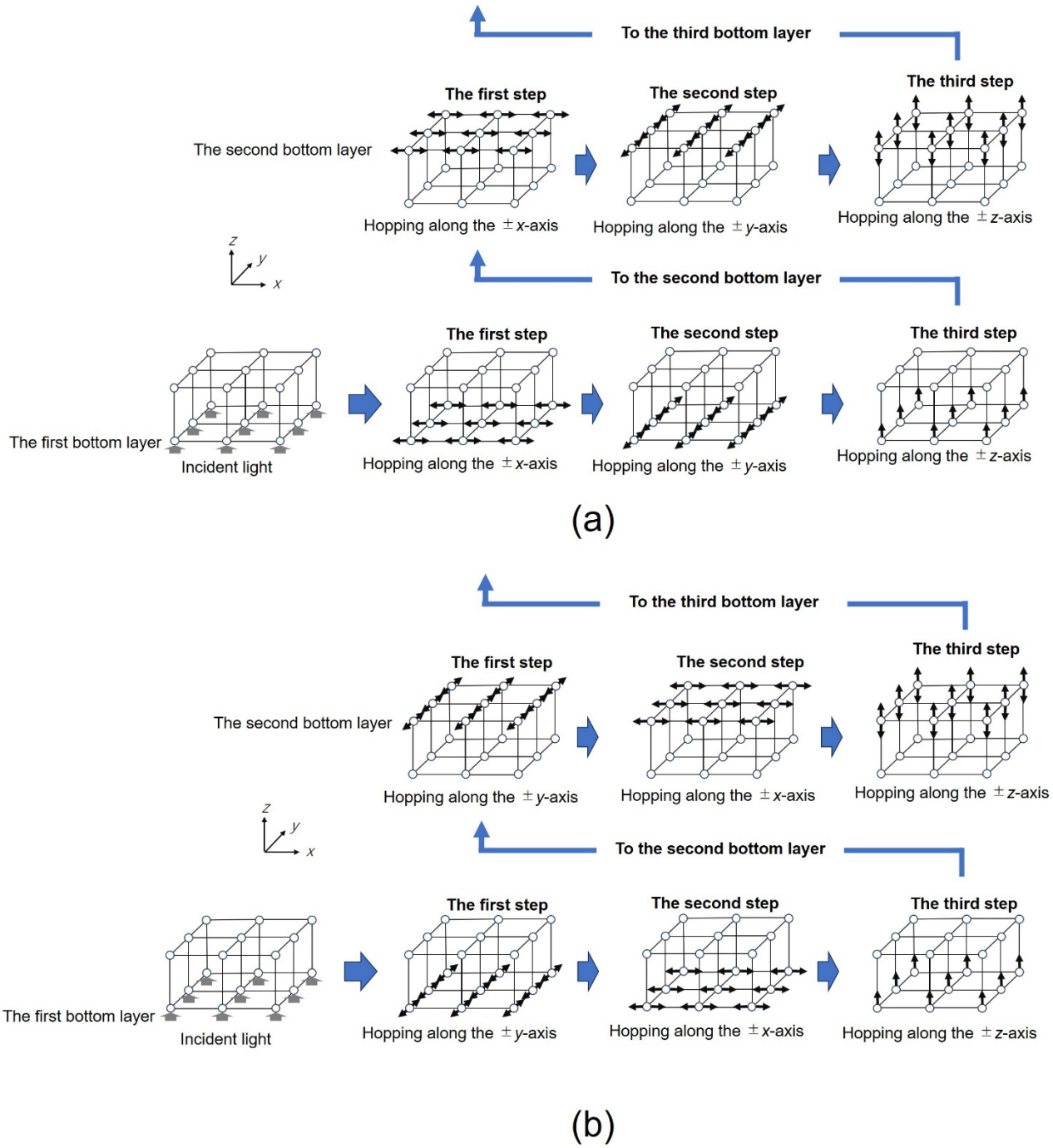

Fig. 6 Direction of the repeated DP hopping at each layer of the three-dimensional lattice.
(a) DP hops along x -, y -, and z -axes at the first, second, and third steps, respectively.
(b) DP hops along y -, x -, and z -axes.

The DPP creation probability at the B atom-pair is given by the square of the absolute value of the DPP state vector, $\left|\vec{\psi}_{t,(x,y)}\right|^2$, as follows:

$$\vec{\psi}_{t,(x,y)} = \begin{bmatrix} y_{DP+} \\ y_{DP-} \\ y_{Phonon} \end{bmatrix}_{t,(x,y)}, \quad (1)$$

where y_{DP+} and y_{DP-} represent the creation probability amplitudes of the DPs that hop in directions parallel and anti-parallel (red and blue arrows in Figs. 3 and 4, respectively) to the propagation direction of the incident light, respectively. y_{Phonon} is the creation probability amplitude of the phonon. The spatial-temporal evolution equations for the state vector $\vec{\psi}_{t,(x,y)}$ have been derived in ref. [12]. These equations are governed by a unitary matrix that is represented by

$$U = \begin{bmatrix} \varepsilon_+ & J & \chi \\ J & \varepsilon_- & \chi \\ \chi & \chi & \varepsilon_0 \end{bmatrix}, \quad (2)$$

where the diagonal elements (ε_+, ε_-, and ε_0) are the eigenvalues of y_{DP+}, y_{DP-}, and y_{Phonon}, respectively [3,4,12]. Off-diagonal elements (J and χ) are DP hopping and DP-phonon coupling energies.

For numerical calculations, the value of J may be set equal to χ ($J = \chi$) at the site of the Si atom. However, at the site of the B atom, χ must be set larger than J ($\chi > J$). This is because the experiments revealed that the B atom serves as a phonon localization center, and thus, such a localized phonon couples with the DP efficiently. In the present article, the ratio χ/J is assumed to be 20 because the previous studies confirmed that the numerically calculated values did not strongly depend on χ / J when $\chi / J \geq 10$ [3]. The number of sites along a side of the three-dimensional lattice is set to 21, and thus, the total number of sites is $(21)^{3*}$. The reflection of the DP at the facets of the lattice is neglected because the side length of the lattice is sufficiently longer than that of the B atom-pair**.

==========

(*) It is known that the number density of the Si atoms in a Si crystal is about 10^{23} (m^{-3}). On the other hand, experiments confirmed that the doping density of B atoms in the Si crystal was about 10^{19} (m^{-3}). The ratio of these is about 10^4. The total number of sites in the lattice $(21)^3$ is nearly equal to this ratio. A super-computer was used to reduce the processing time of the massive amount of calculation data.

(**) The reflection coefficient σ in ref. [12] is set to 0.

==========

4. Calculated results and discussions

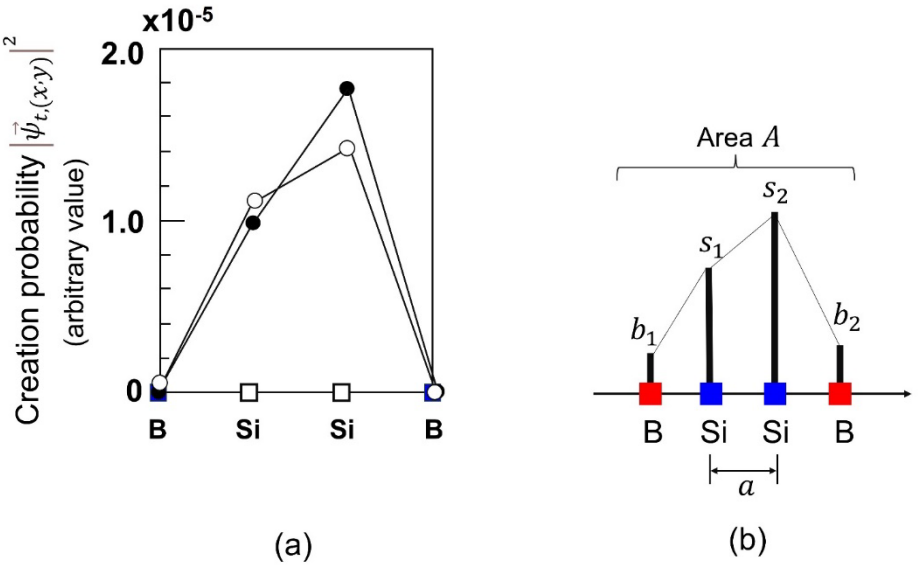

Fig. 7 Calculated stationary values $\left|\vec{\psi}_{t,(x,y)}\right|^2$ of DPP at the B atom-pair.

(a) Closed and open circles represent the calculated value for Figs. 6(a) and (b), respectively.

(b) Schematic definition of the area A.

Figure 7(a) shows calculated stationary values of $\left|\vec{\psi}_{t,(x,y)}\right|^2$ at the B atom-pair. Closed and open circles are the values for the cases of Figs. 6(a) and (b), respectively. Figure 7(b) schematically defines the area A in Fig. 7(a) that is surrounded by the horizontal axis and these circles connected by segments. It is expressed as

$$A = \frac{a}{2}\left[b_1 + 2\left(s_1 + s_2\right) + b_2\right]. \tag{3}$$

By referring to the formula for the degree of polarization P in Section 2, the degree of PB is defined as

$$DoPB = \frac{A_{\rightarrow(z\rightarrow x)} - A_{\uparrow(z\rightarrow y)}}{A_{\rightarrow(z\rightarrow x)} + A_{\uparrow(z\rightarrow y)}}, \tag{4}$$

where $A_{\rightarrow(z\rightarrow x)}$ and $A_{\uparrow(z\rightarrow y)}$ are the areas surrounded by the closed and open circles in Fig. 7(a), respectively. By using Fig. 7(a), eq. (4) derives the value of $DoPB_{\vec{\psi}}$ for $\left|\vec{\psi}_{t,(x,y)}\right|^2$ as 2.0×10^{-2} (=2%).

This positive value indicates that the DPP creation probability in Fig. 1(a) (and Fig. 6(a)) is higher than that in Fig. 1(b) (and Fig. 6(b)). The value 2.0×10^{-2} (=2%) falls in the range of the experimentally evaluated values of P ($0 \le P \le 7\text{x}10^{-2}$ in Section 2). These features indicate PB with respect to the photon spin and confirm that the calculated results above agree with the experimental results. Thus, it is concluded that the goal of the present study, presented at the end of Section 2, was achieved.

Figures 8(a), (b), and (c) show calculated stationary values of $|y_{DP+}|^2$, $|y_{DP-}|^2$, and $|y_{Phonon}|^2$ at the B atom-pair. The values of $DoPB_{DP+}$, $DoPB_{DP-}$, and $DoPB_{Phonon}$ are derived from these figures and eq. (4) and are presented in Table 1. It should be pointed out that y_{DP+} represents the probability amplitude of the DP that hops in the direction parallel to that of the incident light propagation.

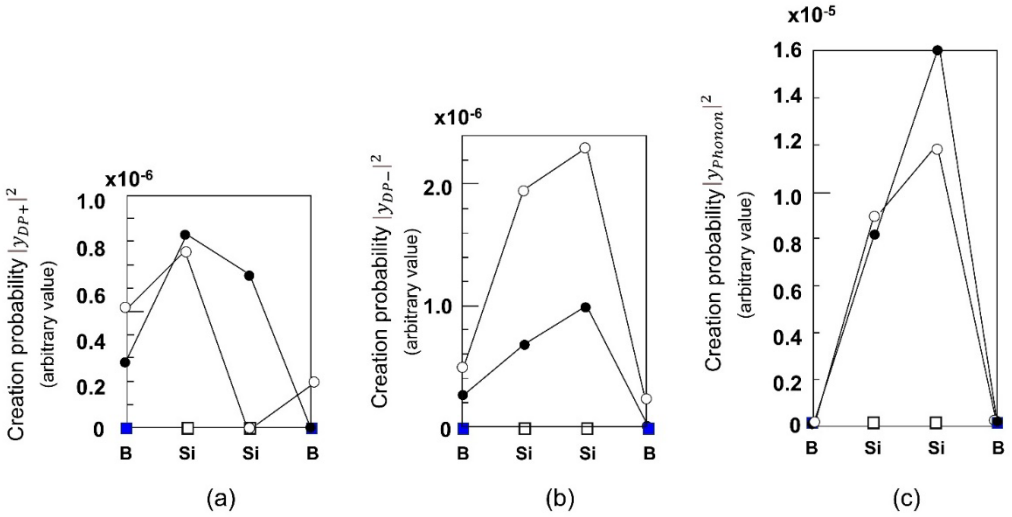

Fig. 8 Calculated stationary values ((a) $|y_{DP+}|^2$, (b) $|y_{DP-}|^2$, and (c) $|y_{Phonon}|^2$) at the B atom-pair for the constituent elements (y_{DP+}, y_{DP-}, and y_{Phonon}) of $\vec{\psi}_{t,(x,y)}$.

Furthermore, the positive $DoPB_{DP+}$ ($DOPB_{DP+} > 0$) in this table indicates that the creation probability of the component y_{DP+} is higher in the case of Fig. 1(a) than of Fig. 1(b). On the other hand, y_{DP-} represents the probability amplitude of the DP that hops in the direction anti-parallel to the that of the incident light propagation. The negative $DoPB_{DP-}$ ($DOPB_{DP-} < 0$) indicates that the

creation probability of the component y_{DP-} is higher in the case of Fig. 1(b). In terms of the absolute value, $DoPB_{DP-}$ is about 2.3 times larger than that of $DoPB_{DP+}$, and $DOPB_{\vec{\psi}}$ takes a positive value (2.0×10^{-2} (=2%)). This again indicates PB with respect to the photon spin and, furthermore, it confirms that the electromagnetic nature of $\vec{\psi}_{t,(x,y)}$ mainly depends on that of y_{DP+}.

Table 1 The calculated values of $DoPB$.

χ / J =20			χ / J =10
$\left\|\vec{\psi}_{t,(x,y)}\right\|^2$	$DoPB_{\vec{\psi}}$ =2.0x10^{-2}(=2.0%)	Fig. 7(a)	$DoPB_{\vec{\psi}}$ =2.3x10^{-2}(=2.3%)
$\left\|y_{DP+}\right\|^2$	$DoPB_{DP+}$ =1.9x10^{-1}(=19%)	Fig. 8(a)	$DoPB_{DP+}$ =1.8x10^{-1}(=18%)
$\left\|y_{DP-}\right\|^2$	$DoPB_{DP-}$ =-4.3x10^{-1}(=-43%)	Fig. 8(b)	$DoPB_{DP-}$ =-4.1x10^{-1}(=-41%)
$\left\|y_{Phonon}\right\|^2$	$DoPB_{Phonon}$ =7.3x10^{-2}(7.3%)	Fig. 8(c)	$DoPB_{Phonon}$ =7.5x10^{-2}(7.5%)

Since the light originated from y_{DP+} propagates in a direction parallel to that of the incident light, and since this parallel propagation feature corresponds to PB with respect to the photon momentum, the indication and confirmation noted above imply that PB with respect to the photon spin and PB with respect to momentum are correlated. Furthermore, this correlation suggests that, if the energy dissipation constant κ in ref. [4] could be introduced into the present three-dimensional QW model in the future, the value of $DoPB_{\vec{\psi}}$ could be evaluated by using the polarization feature of the observable macroscopic light that is emitted from the Si crystal. It is expected that this evaluation could derive a more accurate value of $DoPB_{\vec{\psi}}$ that could be larger than that in Table 1.

The value of χ/J was set to 20 for deriving Figs. 7 and 8, and Table 1 above. As a reference, calculations were carried out also for the case of χ / J =10, and the results confirmed that the spatial distribution profiles of the creation probabilities were almost identical to those in Figs. 7 and 8. Furthermore, the calculated values of $DoPB$ for χ / J =10 were nearly equal to those for the case of χ / J =20, as presented in Table 1. Thus, it was confirmed again that the numerically caclulated values did not strongly depend on χ / J when $\chi / J \geq 10$ [3].

The present study assumed that the direction of the energy transfer of the DP was identical to the propagation direction of the light emitted from the created electric dipole (Figs. 5 and 6). However, it

should be examined more carefully whether this assumption, and also, the explanation using the nanometer-sized wire-grid in (1) of Section 2, are fully acceptable from the viewpoint of nano-science. Future studies based on novel theories of light–matter interactions in a microscopic space [13,14] could find the answers to the fundamental question: "Are these teachings from classical electromagnetics acceptable for describing the phenomena in a nanometer-sized space?".

5. Summary

This article described the features of PB with respect to the photon spin of the light emitted from the Si light-emitting diode by using a three-dimensional QW model. The relation between the direction of the linear polarization of the incident light and DP hopping was assumed by referring to teachings from classical electromagnetics. Numerical calculations found that the DPP creation probability at the B atom-pair depended on the polarization, and the degree of photon breeding was as large as 2%, which agreed with the experimentally confirmed value.

Acknowledgements

The authors thank Dr. S. Sangu (Ricoh corp.) for his valuable comments on building the three-dimensional QW model.

References

[1] Ohtsu, M., Ojima, I., and Sakuma, H., "Dressed Photon as an Off-Shell Quantum Field," Progress in Optics Vol.64, (ed. T.D. Visser) pp.45-97 (Elsevier, 2019).

[2] Ohtsu,M., Off-Shell Applications In Nanophotonics, Elsevier, Amsterdam (2021) p.5.

[3] Ohtsu, M., Segawa, E., Yuki, K., and Saito, S., "Spatial distribution of dressed-photon–phonon confined by an impurity atom-pair in a crystal," Off-shell Archive (January, 2023) OffShell: 2301O.001.v1.,
DOI 10.14939/2301O.001.v1 https://rodrep.or.jp/en/off-shell/original_2301O.001.v1.html

[4] M. Ohtsu, E. Segawa, K. Yuki, and S. Saito, "A quantum walk model with energy dissipation for a dressed-photon–phonon confined by an impurity atom-pair in a crystal," Off-shell Archive (April, 2023) Offshell: 2304O.001.v1.
DOI 10.14939/2304O.001.v1 https://rodrep.or.jp/en/off-shell/original_2304O.001.v1.html

[5] M. Ohtsu, Silicon Light-Emitting Diodes and Lasers (Springer, Heidelberg, 2016) pp.1-120.

[6] M. Ohtsu, Silicon Light-Emitting Diodes and Lasers (Springer, Heidelberg, 2016) pp.35-39.

[7] T. Kawazoe, K. Nishioka, and M. Ohtsu, "Polarization control of an infrared silicon light-emitting diode by dressed photons and analyses of the spatial distribution of doped boron atoms," *Applied Physics A*, Vol.121, Issue 4, December 2015, pp.1409-1415.

[8] M. Ohtsu, Silicon Light-Emitting Diodes and Lasers (Springer, Heidelberg, 2016) pp.39-42.

[9] M. Yamaguchi, T. Kawazoe, and M. Ohtsu, "Evaluating the coupling strength of electron–hole pairs and phonons in a 0.9 μm-wavelength silicon light emitting diode using dressed-photon–phonons," Appl. Phys. A, Volume 115, Issue 1, April 2014, pp. 119-125.

[10] N. Wada, M. A. Tran, T. Kawazoe, and M. Ohtsu, "Measurement of multimode coherent phonons in nanometric spaces

in a homojunction-structured silicon light emitting diode," Appl. Phys. A, Volume 115, Issue 1, April 2014, pp. 113-118.
[11] M. Ohtsu, Silicon Light-Emitting Diodes and Lasers (Springer, Heidelberg, 2016) pp.43-63.

[12] M. Ohtsu, "A Quantum Walk Model for Describing the Energy Transfer of a Dressed Photon," *Off-shell Archive* (September, 2021) OffShell: 2109R.001.v1. **DOI** 10.14939/2109R.001.v1, http://offshell.rodrep.org/?p=345

[13] H. Sakuma, I. Ojima, M. Ohtsu, and H. Ochiai, "Off-Shell Quantum Fields to Connect Dressed Photons with Cosmology," Symmetry, vol.12, no.8 (2020) 1244. DOI:10.3390/sym12081244

[14] H. Sakuma, I. Ojima, M. Ohtsu and T. Kawazoe, "Drastic advancement in nanophotonics achieved by a new dressed photon study," *JEOS-RP* (2021)**17**:28.
https://jeos.springeropen.com/articles/10.1186/s41476-021-00171-w